

MODELLING OF THE ORGANISED MOTION IN TURBULENT FLOWS

D.K. BISSET and R.A. ANTONIA

Department of Mechanical Engineering
 University of Newcastle, NSW 2308
 AUSTRALIA

ABSTRACT

Groups of modified Rankine vortices are used to model the organised motion in the turbulent plane self-preserving far-wake of a cylinder. Reynolds stresses $\overline{u^2}$, $\overline{v^2}$ and \overline{uv} are reproduced quite well. A quasi-three-dimensional version of the model implies that large spanwise vortices and shear-aligned double rollers are actually the same three-dimensional organised motion from two different viewpoints.

INTRODUCTION

Townsend's (1956) monograph was instrumental in drawing widespread attention to the role of an organised motion, usually of large scale, in a turbulent shear flow. One of the techniques that Townsend used to evaluate the importance of this motion was to propose kinematic models, such as various kinds of eddies or vortices, and compare measured flow properties such as correlation coefficients with the model's predictions. The same basic idea is used here, but extended by means of a digital computer into a more versatile and more interactive process in which improvements in the model can suggest new aspects to study in experimental data, the result of which can improve the model, and so on.

The flow considered here is the turbulent plane self-preserving far-wake of a cylinder (see Figure 1 for a definition sketch). The Reynolds decomposition is used, e.g. the instantaneous longitudinal velocity $U = \overline{U} + u$, the mean and fluctuating components respectively. The distributions of kinematic Reynolds normal stresses ($\overline{u^2}$ and $\overline{v^2}$) and shear stress (\overline{uv}), are of particular interest. Assuming that data are in the form of a digital time series, detections are defined as the time instants t_j , $j = 1, \dots, n$ when a certain feature related to the organised motion occurs. Conditional averages of some quantity

$$(u, \text{ for example}) \text{ are defined as } \langle u \rangle_k = \frac{1}{n} \sum_{j=1}^n u(t_j + k)$$

where k is time (in samples) relative to the detection instants. (Usually the subscript k is omitted). This leads to the triple decomposition, e.g. $U = \overline{U} + \langle u \rangle + u_r$, where u_r is that part of u not correlated with the detected feature of the flow. From this, $\langle u^2 \rangle = \langle u \rangle^2 + \langle u_r^2 \rangle$, $\langle uv \rangle = \langle u \rangle \langle v \rangle + \langle u_r v_r \rangle$ and so on. Given a suitable detection set, $\langle uv \rangle_k$ is a strong function of k , although the average value of $\langle uv \rangle_k$ for an appropriate range of k (e.g. one period of the organised motion) may be equal to \overline{uv} . Analogous statements apply for $\overline{u^2}$ and $\overline{v^2}$. One could find, however, that the organised motion is "organising" the Reynolds stresses without actually creating them, e.g. $\langle u_r v_r \rangle \approx \langle uv \rangle$ and $\langle u \rangle \langle v \rangle \approx 0$, although measured values of $\langle u \rangle \langle v \rangle$ are often significant (e.g. Antonia et al., 1987a). The question addressed here is: can the organised motion be modelled such that it creates virtually all of the Reynolds stresses?

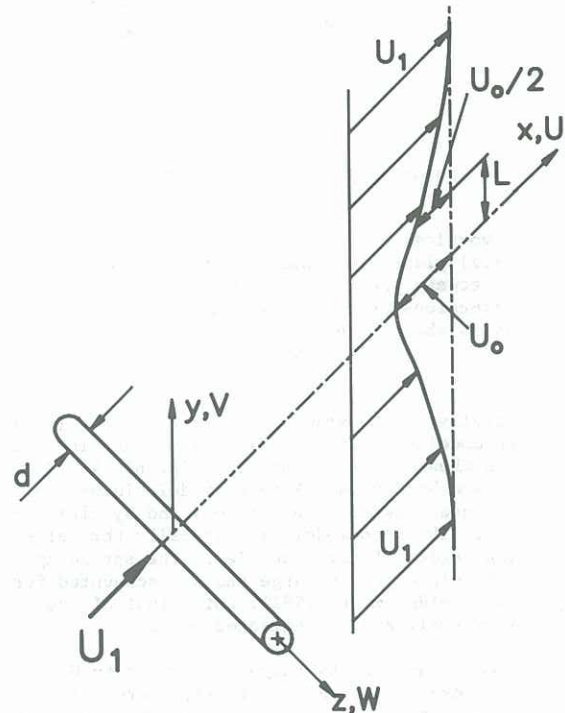


Figure 1 Definition sketch

Data from experiments in the far-wake of a cylinder at a Reynolds number $R_d = 1200$ and $x/d = 420$ are available for comparison with the results of modelling. Figure 2 shows sectional streamlines (Perry and Chong, 1987) calculated from a small part of the digital data obtained using a rake of eight X-probes, aligned parallel to the y -axis, measuring u and v . Time has been converted to distance using $\Delta x = -U_c \Delta t$, where U_c is the frame-of-reference velocity. In another experiment the probes were aligned with the z -axis measuring u and w . At the instant shown in Figure 2, there is a pattern of unstable foci and saddles (see Perry and Chong, 1987) alternating about the centreline, but at other instants there is a nearly symmetrical pattern with a focus opposite a focus across the centreline of the wake. The apparent distances of foci and saddles from the centreline can vary considerably. The regions separated in x by successive saddles, each containing a large focus, can be identified with large spanwise vortices, and it is clear that they fill most of the wake. Another kind of dominant structure has been proposed, however, containing a series of single or double rollers with axes aligned roughly parallel to the y -axis (Grant, 1958; Mumford, 1983). The modelling carried out in this paper is based on large

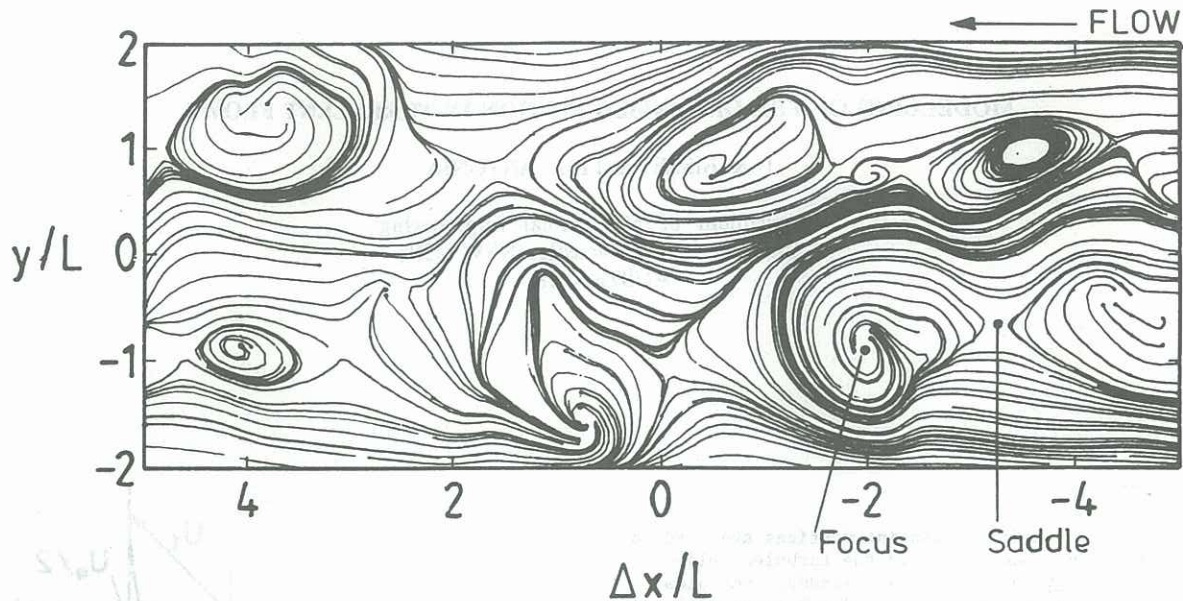


Figure 2 Instantaneous sectional streamlines from experimental data in a frame of reference translating at $U_c = U_1 - 0.5U_0$.

spanwise vortices, yet the velocity patterns implied in the (x, z) plane are consistent with double rollers. The link between the two types of structure is $\langle u \rangle \langle v \rangle$, the contributions of the large spanwise vortices to the Reynolds shear stress.

METHOD

Initially, large spanwise vortices in the (x, y) plane are modelled. The two-dimensional Rankine line vortex was chosen as the basic building block. It has been used by Davies (1976) to model kinematically the planar near-wake of a bluff body and by Oler and Goldschmidt (1982) to model kinematically the self-preserving region of the plane jet. The spreading rate of the plane jet is large and was accounted for by Oler and Goldschmidt (1982), while that of the far-wake is small and is neglected here.

The equation for the tangential velocity U_θ is $U_\theta = \Gamma \{1 - \exp[-1.26(r/R_0)^2]\} / (2\pi r)$, where Γ is the circulation, r the radial position, and R_0 the cutoff radius (where U_θ is maximum). The unit of length is the mean velocity half-width L , and velocities are scaled so that $U_0 = 1$. A computer program places a number of vortices at specified (x_c, y_c) locations within (or adjacent to) a two-dimensional computational grid, superimposes U and V components of U_θ for each vortex at each grid point, and then calculates \bar{U} , \bar{V} , \bar{u}^2 , \bar{v}^2 and \bar{uv} as a function of y . For example, $\bar{u}^2 = (1/p) \sum_{i=1}^p (U_i - \bar{U})^2$ where the computa-

tional field is p points long (typically 12 points per vortex). The rows of vortices are always extended beyond the computational field so that the data are equivalent to continuous flow. For the results presented here, the longitudinal spacing λ is always equal to the experimental value of 3.0, $|\Gamma|$ is 5.0 (arbitrary) and R_0 is 1.0 for all vortices. The mean transverse velocity \bar{V} is ignored as it is always many orders smaller than \bar{U} .

RESULTS

The first model was a series of vortices, with circulation of alternate sign, placed alternately across the centreline at $|y_c| = 0.8$ (Figure 3a). $\bar{U}(y)$ was correct but the Reynolds stresses were quite wrong, especially \bar{uv} which was virtually zero everywhere. The second model was similar except

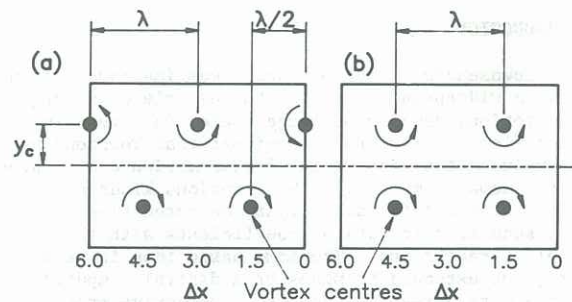


Figure 3 Positions of vortex centres for (a) the first model, and (b) the second model. Vortices outside the computation domain are not shown.

that the vortices were placed opposite each other (Figure 3b), but again the stresses were incorrect.

In Bisset et al. (1989), regions of experimental data with either alternating or opposing arrangements of detections were analysed separately, showing differences in the way they contribute to mean Reynolds stresses. A similar idea was adopted for the third and subsequent models. The third model was simply the sum of the previous two, in the sense that mean velocity and Reynolds stress profiles were linear combinations of the profiles from the two arrangements of vortices, e.g.

$$\bar{u}^2 = \beta \bar{u}^2_{\text{alternate}} + (1-\beta) \bar{u}^2_{\text{opposite}}$$

Values of β in the range 0.6 to 0.7 are indicated by the experimental results (Bisset et al., 1989). With $\beta = 0.67$, the third model predicts the \bar{v}^2 profile quite accurately, but the \bar{u}^2 profile is poor and \bar{uv} is still zero.

Velocity fluctuations u and v measured in the potential flow just outside a turbulent wake by Antonia et al. (1987b) were found to be 90° out of phase. The same result is obtained from the Rankine vortex models, which is the reason why \bar{uv} is zero. Within a turbulent shear flow, however, the phase relationship is generally nearer to 0° or 180° (e.g. Antonia et al., 1986), and this aspect was addressed by the fourth model. A phase lag ϕ was introduced into the computation of U , i.e. $U = -U_0 \sin(\theta - \phi)$,

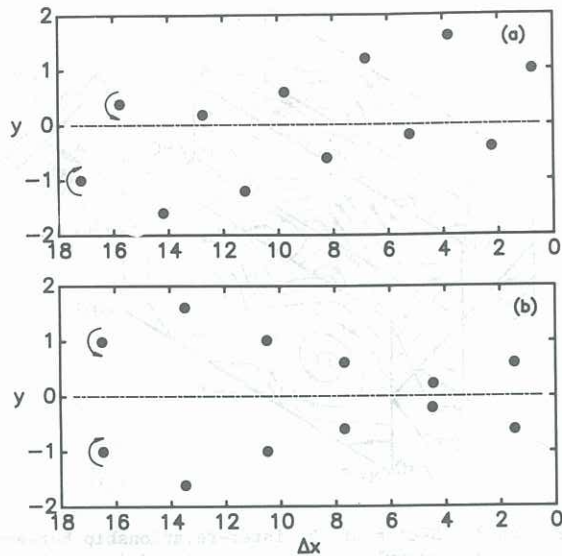


Figure 4 Positions of vortex centres for the fifth model. (a) alternating pattern; (b) opposing pattern. Vortices outside the computation domain are not shown.

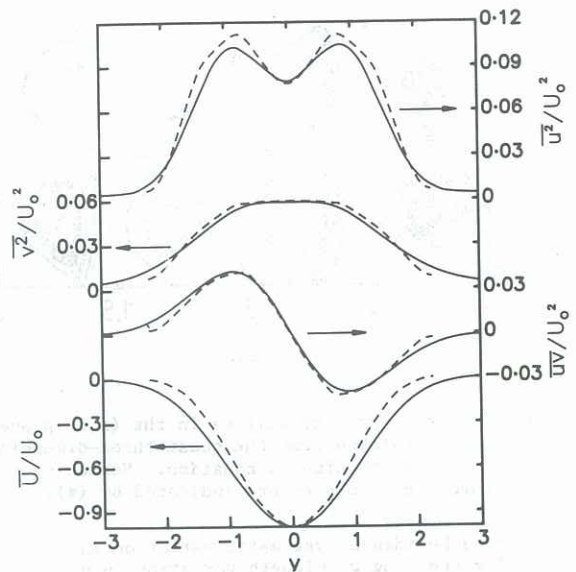


Figure 5 Profiles of mean velocity and Reynolds stresses from the fifth model (—), compared with experimental results (---).

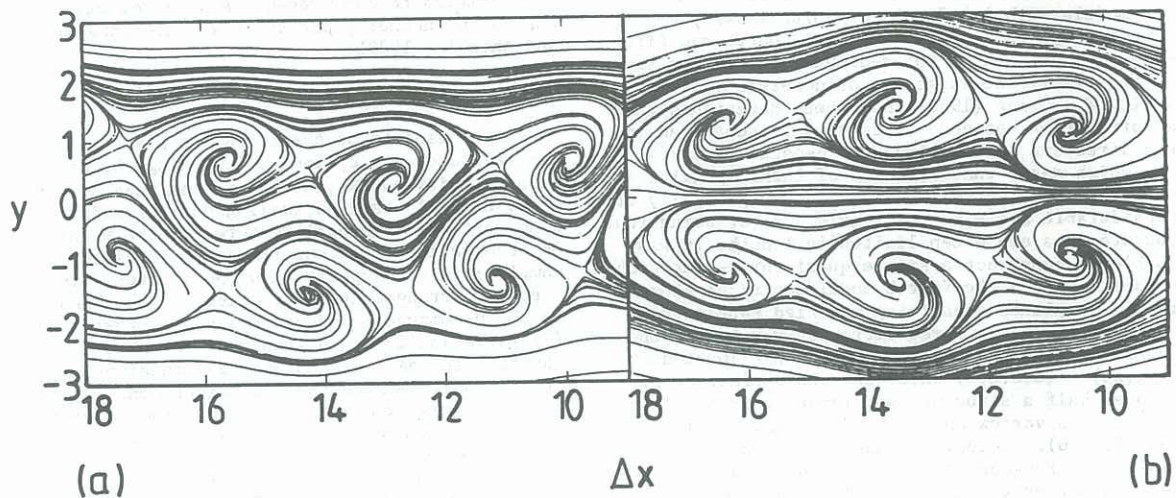


Figure 6 Sectional streamlines calculated from half of the vortices shown in Figure 4 with a frame of reference convection velocity $U_c = U_1 - 0.5U_0$. (a) alternating pattern; (b) opposing pattern. The model uses, in effect, two parts of (a) to one part of (b).

while $V = U_0 \cos \theta$ as before, where $\theta = \tan^{-1}[(y-y_c)/(x-x_c)]$ for a given point (x,y) . The sign of ϕ depends on the sign of Γ , and for $r > R_0$ the value of ϕ is proportional to $(R_0/r)^2$ so that the phase lag occurs only in the "turbulent" zones. The phase lag is applied to U rather than V because it is found in the experimental data that detections in v signals from adjacent probes generally occur at the same time while detections in u signals occur consistently at different times. The fourth model also allows for an additional vortex convection velocity (U_{cc}, V_{cc}) to be applied to the inner regions of the vortices (where $r < R_0$), and reduced in proportion to $(R_0/r)^2$ elsewhere, but (U_{cc}, V_{cc}) is not as important as ϕ . It was found that with $\phi = 35^\circ$ and $(U_{cc}, V_{cc}) = (0.19, 0.0)$ the profiles of \bar{U} , \bar{v}^2 and \overline{uv} were reproduced very well, but \bar{u}^2 values were still very low. Sectional streamlines computed for this model (similar to Figure 6) show the correct pattern of foci and saddles (cf. Figure 2), unlike streamlines from the first three models which showed patterns of centres and saddles.

The apparent distances of large structures from

the centreline vary considerably (cf. Figure 2), and the conventional auto-correlation coefficient for u remains positive up to large x (Grant, 1958). The fifth model accounts for these two aspects by systematically varying y_c over groups of six vortices per side, with $0.2 \leq |y_c| \leq 1.5$ (average 0.8). The variation is antisymmetrical for the group of alternating vortices (Figure 4a) and symmetrical for the opposing group (Figure 4b). The resulting velocity and stress profiles, for parameter values of $\phi = 45^\circ$, $\beta = 0.6$ and $U_{cc} = 0.06$, are compared with measurements (Antonita et al., 1987a) in Figure 5, and agreement is very good, especially for \bar{v}^2 and \overline{uv} . Note that the profiles for \bar{u}^2 and \bar{v}^2 from the alternating and opposing groups taken separately are quite different, and it is only their combinations that are close to the experimental results. The corresponding sectional streamlines for part of the data are shown in Figure 6. It can be inferred from these results that a long wavelength variation in u , of a scale larger than the largest vortex-like structures, is responsible for both the long positive tail in the measured auto-correlation coefficient and a considerable proportion of the measured \bar{u}^2 . However, there may be

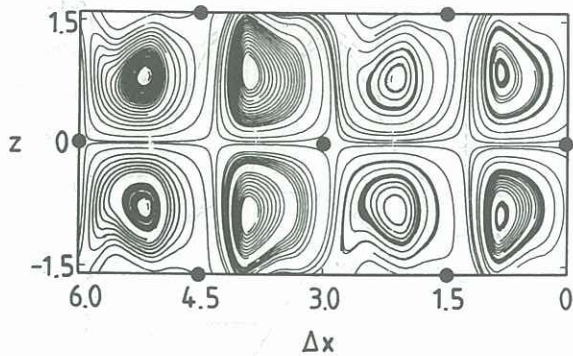


Figure 7 Sectional streamlines in the (x,z) plane at $y = 1.0$ calculated from the quasi-three-dimensional model via the continuity equation. Vortex centres in the three (x,y) planes are indicated by (\bullet) .

other ways besides a systematic variation in y_c of modelling the long wavelength variation in u .

Although the mean flow is two-dimensional, the magnitude of the divergence $\partial U/\partial x + \partial V/\partial y$ is often significant in the experimental data. The divergence for the first three models was everywhere zero, but significant values were found for the fourth and fifth models with $\phi \neq 0$. Since $\partial U/\partial x + \partial V/\partial y = -\partial W/\partial z$ for incompressible flow, the fourth and fifth models are, therefore, three-dimensional in the sense that they imply the existence of non-zero spanwise velocity W . Grant (1958) and others have found that the correlation between u measurements separated in the z direction is significantly negative at $\Delta z \approx 1.6L$, which means that the axes of large spanwise structures are limited in length and/or generally at a considerable angle to the z -axis. By assuming that structure axes are often limited in length, it was possible to construct a simple quasi-three-dimensional model based on the fourth model described above. Three (x,y) planes containing modified Rankine vortices were placed at three different z values. One plane was aligned so that one vortex was located at $(x_c, y_c, z_c) = (0, 0.8, 0)$ while the other planes were displaced half a structure wavelength in x and $\pm 1.6L$ in z , i.e. a vortex was centred at $(x_c, y_c, z_c) = (1.5, 0.8, \pm 1.6)$. Velocity components U and V were calculated throughout the three planes, and then calculated at other z values by linear interpolation between the planes. (The implied physical picture is a pattern of interlocking spindle shapes rotating about axes of length $3.2L$ parallel to the z -axis). It was assumed that the $(x,y,0)$ plane was a plane of symmetry, i.e. $W = 0$ in this plane, and then W was calculated elsewhere by numerical integration of $\partial W = -(\partial U/\partial x + \partial V/\partial y)\partial z$.

Sectional streamlines calculated from U and W in the plane $(x, 1.0, z)$ are shown in Figure 7 in a frame-of-reference moving with the mean velocity of that plane. Very similar results were obtained over a large range of y -values provided that the local \bar{U} was used for the frame-of-reference velocity. The pattern in Figure 7 conforms remarkably well to the concept of counter-rotating double rollers with axes nearly normal to the centreplane of the wake proposed by Grant (1958) and Mumford (1983). The relationship between the (x,z) plane of Figure 7 and the three (x,y) planes from which it was generated is shown in Figure 8. Three-dimensional streamlines resulting from this data would be quite complex. Note that the double roller pattern does not appear when the U phase delay ϕ is zero, i.e. the model implies that spanwise vortices and double rollers are interlinked through the Reynolds shear stress associated with the large scale organised motion.

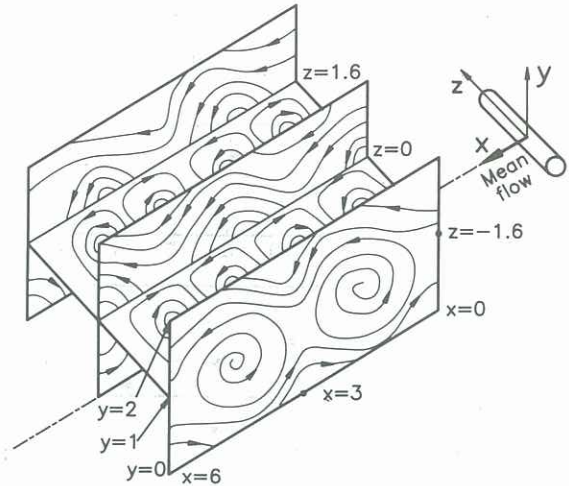


Figure 8 Sketch of the inter-relationship between sectional streamlines in the (x,y) and (x,z) planes for the quasi-three-dimensional model. Only the upper half of the wake is shown.

Conditional averages from experimental data in both (x,y) and (x,z) planes show certain remarkable similarities to the present results and will be discussed in another paper at this conference (Bisset and Antonia, 1989).

CONCLUSIONS

Many aspects of the turbulent plane self-preserving far-wake of a cylinder, including the profiles of mean velocity and Reynolds stresses, can be reproduced by a model based on small groups of modified Rankine vortices. Several features of the model, based on observations from experiments, are essential, namely: (a) incorporation of both alternating and opposing arrangements of vortices; (b) a phase delay in the U component induced by each vortex; and (c) variation in the distance of vortex centres from the centreplane. A quasi-three-dimensional version of the model implies that two experimentally observed types of organised motion (large spanwise vortices, and single or double rollers) are actually the same underlying structure seen from two different viewpoints. Reynolds shear stress induced by the organised motion is the linking factor.

ACKNOWLEDGEMENTS

Assistance with experiments by Dr L. W. B. Browne, and financial assistance from the Australian Research Council, are gratefully acknowledged.

REFERENCES

- ANTONIA, R. A., BROWNE, L. W. B., BISSET, D. K. and FULACHIER, L. : 1987a. *J. Fluid Mech.*, **184**, 423.
 ANTONIA, R. A., CHAMBERS, A. J., BRITZ, D. H. and BROWNE, L. W. B. : 1986. *J. Fluid Mech.*, **172**, 211.
 ANTONIA, R. A., SHAH, D. A. and BROWNE, L. W. B. : 1987b. *Phys. Fluids*, **30**, 2040.
 BISSET, D. K. and ANTONIA, R. A. : 1989. *Proc. Tenth Australasian Fluid Mechanics Conference*, Melbourne.
 BISSET, D. K., ANTONIA, R. A. and BROWNE, L. W. B. : 1989. *J. Fluid Mech.* [submitted].
 DAVIES, M. E. : 1976. *J. Fluid Mech.*, **75**, 209.
 GRANT, H. L. : 1958. *J. Fluid Mech.*, **4**, 149.
 MUMFORD, J. C. : 1983. *J. Fluid Mech.*, **137**, 447.
 OLER, J. W. and GOLDSCHMIDT, V. W. : 1982. *J. Fluid Mech.*, **123**, 523.
 PERRY, A. E. and CHONG, M. S. : 1987. *Ann. Rev. Fluid Mech.*, **19**, 125.
 TOWNSEND, A. A. : 1956. *The Structure of Turbulent Shear Flow*, 1st ed., Cambridge, C.U.P.